



Numerical Algebra Solution: A New Algorithm for the State Transition Matrix

Wenfeng Nie^{a,b}, Tianhe Xu^{a,b,*}, Yujun Du^a, Fan Gao^a, Guochang Xu^a

^a Institute of Space Sciences, Shandong University, Weihai 264209, PR China

^b State Key Laboratory of Geo-information Engineering, Xi'an 710054, PR China

Received 29 August 2016; received in revised form 18 January 2017; accepted 27 February 2017

Abstract

A new algorithm named the numerical algebra solution for the state transition matrix is proposed in this paper. The objective of the solution is to yield a comparable accuracy of the trajectory at the least computational cost. To validate it, the time consumption and accuracy performance of the numerical algebra solution are compared with those of the numerical integration and difference quotient method for both the real-time and post-processed orbit determination. Simulation results with the measurement noise only show that the time consumption of the numerical algebra solution accounts for about 60% and 40% of the numerical integration method for the real-time and post processing, respectively. Furthermore, the maximum position RMS difference of the numerical algebra solution with respect to the numerical integration method is about 1.04 mm and 0.01 mm for the real-time and post processing, while the position error of the numerical integration method is about 1.20 m and 0.30 mm, respectively. These accuracy performances demonstrate that the difference between the numerical algebra and integration solution is indistinguishable and can be accepted in the orbit determination. Advantageously, the numerical algebra solution can improve the computational efficiency greatly, which is particularly important for the real-time orbit determination.

© 2017 COSPAR. Published by Elsevier Ltd. All rights reserved.

Keywords: Numerical algebra solution; State transition matrix; Variational equation; Time consumption

1. Introduction

The solution of the state transition matrix (STM) is a necessity in the orbit determination, not only because it relates the state of the satellite from current to initial time but also because it propagates the covariance of the state (Battin, 1964; Liu, 2000; Montenbruck and Gill, 2000; Tapley et al., 2004a). Theoretically, if the initial state and forces acting on the satellite are precisely known, the precise orbit can be computed by integration methods. In practice, however, neither the initial state nor the forces

acting on the satellite can be known accurately before orbit determination (Xu, 2007; Xu and Xu, 2013). Therefore, observations from different geodetic techniques, such as Global Navigation Satellite System (GNSS) or Doppler Orbitography and Radio-positioning Integrated by Satellite (DORIS), should be applied to determine these parameters (Tapley et al., 1994; Willis et al., 2003, 2010; Jin, 2012). During the orbit determination, STM plays an important role in both the observation and state equation, through which the initial state and force model parameters can be calculated precisely.

The determination of STM has two outstanding characteristics (Montenbruck and Gill, 2000). Firstly, the calculation of STM is one of the highest computational cost procedures in the orbit determination. The reason is that

* Corresponding author at: Institute of Space Sciences, Shandong University, Weihai 264209, PR China.

E-mail address: thxugie@163.com (T. Xu).

the calculation of the partial derivatives of the acceleration with respect to the state and force model parameters requires the highest amount of computational burden. Besides, the STM is usually used in an iterative manner, which also increases the computation time (Mueller, 1977). Secondly, the accuracy requirement for STM solution is more relaxed than that for the trajectory, because STM itself is a liner approximation term in a Taylor series expansion of the state vector at current time related to the state vector at the initial time (Tapley et al., 2004a).

Aimed at these two features, numerous methods are proposed to compute STM in some previous researches, which include the various analytical formulas, numerical differentiation and integration methods (Ditto, 1969; Broucke, 1970; Der, 1997; Liu, 2000; Ramachandran, 2015). In terms of the analytical methods, a completely general closed-form solution for STM of the two-body problem is proposed by Goodyear (1965), which was suitable for any kind of conic motion and recognized as a definitive work in the area of analytical solutions. Based on Goodyear's method, Shepperd (1985) enhanced the method by using the universal variable which required the evaluation of only one transcendental function. Though the above two methods were complete and elegant, they were based on the assumption that all perturbations were not considered, which may cause non-negligible effects when the perturbations were large. To cope with this problem, a solution, which include the secular as well as the long- and short-period effects of planetary oblateness, was analyzed by Born and Kirkpatrick (1970). Results demonstrated that this method improved the accuracy of STM three to four orders of magnitude over the two-body model. The advantage of the analytical methods is their high computational efficiency, but the complex force model expression poses restrictions on the accuracy of the analytical methods.

However, for the numerical methods, such as integration and difference quotient method, the situations are quite different. The numerical integration method, such as the Runge-Kutta method and Adams method, is recognized as the most accurate method and always taken as a reference to the other methods (Beutler, 2004; Tapley et al., 2004a). But the computer implementation of the corresponding formulas is quite complex and laborious because the computation of partial derivatives of the acceleration with respect to the state should be dealt with seriously, especially for the partial derivative of the gravity acceleration with respect to the state, though some common sub-expressions are already computed as a result of computing the acceleration (Montenbruck and Gill, 2000). Besides, the partial derivatives have to be computed for not once, but a few times in a certain step-size according to the order of the integration method. In order to reduce the complexity of the integration formulas, numerical difference quotient method is a good choice, because the algorithm avoids the computation of the partial derivatives (Hu et al., 2000). A typical application of the differ-

ence quotient method is to compute the partial derivative of the atmosphere drag acceleration with respect to the state, while the integration method cannot work due to the non-availability of an appropriate analytical formulation (Montenbruck and Gill, 2000). However, one major disadvantage of the difference quotient method lies in the difficulty of selecting a proper initial parameter increment, which is critical to minimize the overall error of the solution. Moreover, owing to the fact that the common sub-expressions have already calculated for the acceleration and then stored, the expense of the numerical difference quotient method is thought to be larger than that of the numerical integration method according to Montenbruck and Gill (2000).

To address the aforementioned problems, a new algorithm for STM, namely the numerical algebra solution, is presented in this paper. The objective of the solution is to yield a comparable accuracy of the orbit at the least computational cost. In order to assess the performance of the proposed method, the computational cost and accuracy of the solution are compared with those of the numerical integration and difference quotient method, while the analytical methods are not considered in this paper.

The paper is presented as follows. In Section 2, the variational equation as well as the concept of STM is introduced. Then the numerical methods are presented in Section 3 with emphasis on the numerical algebra solution. The validation methodology and comparison results are shown in Sections 4 and 5, respectively. Finally, some conclusions are drawn in Section 6.

2. The state transition matrix

The concept of STM can be deduced from Newton's second law. In an inertial Cartesian coordinate system, the perturbed equation of satellite motion can be described by Newton's second law as

$$\ddot{\vec{r}} = \vec{f}/m \quad (1)$$

where $\ddot{\vec{r}}$ is the acceleration of the satellite with mass m and \vec{f} is the vector sum of all the forces acting on the satellite.

Eq. (1) is a second-order differential equation. For convenience, it can be written as two first-order differential equations as follows

$$\frac{d\vec{r}}{dt} = \vec{r} \quad \frac{d\vec{r}}{dt} = \frac{\vec{f}}{m} \quad (2)$$

where \vec{r} and $\dot{\vec{r}}$ are the position and velocity vector of the satellite, respectively.

Denoting $\vec{X} = (\vec{r} \ \dot{\vec{r}})^T$ and $\vec{F} = (\vec{r} \ \dot{\vec{r}}/m)^T$ with superscript T the transpose of row vector to column vector, Eq. (2) can be rewritten as

$$\dot{\vec{X}} = \vec{F} \quad (3)$$

Eq. (3) is called the state equation of satellite motion. Taking the partial derivatives of the satellite state equation at time t with respect to the initial state, as well as the parameter vector of force models, we get the variational equation as follows

$$\frac{\partial \vec{X}(t)}{\partial (\vec{X}(t_0), \vec{p})} = \frac{\partial \vec{F}(t)}{\partial (\vec{X}(t_0), \vec{p})} = \frac{\partial \vec{F}(t)}{\partial \vec{X}(t)} \frac{\partial \vec{X}(t)}{\partial \vec{X}(t_0)} + \frac{\partial \vec{F}(t)}{\partial \vec{p}} \quad (4)$$

where $\vec{X}(t_0) = (\vec{r}(t_0), \vec{v}(t_0))^T$ is the initial state and \vec{p} represents the parameter vector of different forces acting on the satellite.

In Eq. (4), $\frac{\partial \vec{X}(t)}{\partial \vec{X}(t_0)}$ is the so-called state transition matrix,

which is the sensitivity of the current state $\vec{X}(t)$ of the orbiting body with respect to its state at the initial epoch $\vec{X}(t_0)$ (Tapley et al., 2004a; Junkins et al., 2008).

To be convenient, Eq. (4) can be expressed in the following form as

$$\dot{\Phi}(t, t_0) = D(t)\Phi(t, t_0) + C(t) \quad (5)$$

with

$$\Phi(t, t_0) = \frac{\partial \vec{X}(t)}{\partial \vec{X}(t_0)}, \quad D(t) = \frac{\partial \vec{F}(t)}{\partial \vec{X}(t)} \quad \text{and} \quad C(t) = \frac{\partial \vec{F}(t)}{\partial \vec{p}} \quad (6)$$

In Eq. (5), $\Phi(t, t_0)$ is the state transition matrix and $C(t)$ is the differential equation of the sensitivity matrix while $D(t)$ is the design matrix which is related to the partial derivative of the satellite acceleration with respect to the state.

3. Numerical solutions of STM

The numerical solutions include the integration, difference quotient and algebra method in this paper. Among them, the integration method is the most widely used in the process of orbit determination. In this case, the RK4 numerical integrator (Runge-Kutta of order 4) for real-time and RKF78 integrator (Runge-Kutta with Fehlberg coefficients of order 7–8) for post-processed orbit determination are employed. Detailed descriptions of the integration method can be found in many textbooks relating to the satellite orbit determination, such as Liu (2000), Montenbruck and Gill (2000), as well as Xu and Xu (2013), thus the content of the numerical integration algorithm is not presented in this paper.

3.1. Numerical algebra solution

The key point of the numerical algebra solution is the applying of the rule of the symmetric derivative under the limit, also known as the rule of symmetric difference quotient, to calculate the STM (Peter and Maria, 2014).

According to the definition, the STM is the partial derivative of the current state with respect to the initial

state, thus it can be divided into two parts, where the up part $\psi(t, t_0)$ and the down part $\dot{\psi}(t, t_0)$ are the partial derivative of the position and velocity component with respect to the initial state, respectively. In the same way, $\ddot{\psi}(t, t_0)$ is the partial derivative of the acceleration component with respect to the initial state, which is shown as follows

$$\Phi(t, t_0) = \begin{pmatrix} \psi(t, t_0) \\ \dot{\psi}(t, t_0) \end{pmatrix}, \quad \dot{\Phi}(t, t_0) = \begin{pmatrix} \dot{\psi}(t, t_0) \\ \ddot{\psi}(t, t_0) \end{pmatrix} \quad (7)$$

As for the differential equation of the sensitivity matrix $C(t)$ and the design matrix $D(t)$ in Eq. (5), they can be expanded as

$$D(t) = \frac{\partial \vec{F}(t)}{\partial \vec{X}(t)} = \begin{pmatrix} 0_{3 \times 3} & E_{3 \times 3} \\ \frac{1}{m} \frac{\partial \vec{f}}{\partial \vec{r}} & \frac{1}{m} \frac{\partial \vec{f}}{\partial \vec{v}} \end{pmatrix} \quad (8)$$

$$C(t) = \frac{\partial \vec{F}(t)}{\partial \vec{p}} = \begin{pmatrix} 0_{3 \times 6} & 0_{3 \times n_p} \\ 0_{3 \times 6} & \frac{1}{m} \frac{\partial \vec{f}}{\partial \vec{p}} \end{pmatrix}$$

where E is an identity matrix and n_p is the dimension of the force model parameter vector. Denoting

$$A(t) = \frac{1}{m} \frac{\partial \vec{f}}{\partial \vec{r}}, \quad B(t) = \frac{1}{m} \frac{\partial \vec{f}}{\partial \vec{v}} \quad \text{and} \quad G(t) = \frac{1}{m} \frac{\partial \vec{f}}{\partial \vec{p}} \quad (9)$$

Eq. (8) can be written in the following simplified form as

$$D(t) = \begin{pmatrix} 0_{3 \times 3} & E_{3 \times 3} \\ A(t) & B(t) \end{pmatrix} \quad C(t) = \begin{pmatrix} 0_{3 \times 6} & 0_{3 \times n_p} \\ 0_{3 \times 6} & G(t) \end{pmatrix} \quad (10)$$

Therefore, combining Eq. (7) with (10), the alternate expression of Eq. (5) can be obtained as:

$$\frac{d^2 \psi(t, t_0)}{dt^2} = A(t)\psi(t, t_0) + B(t) \frac{d\psi(t, t_0)}{dt} + G(t) \quad (11)$$

As Eq. (11) is an equation system of size $3 \times (6 + n_p)$ and $A(t)$ and $B(t)$ are 3×3 matrices, Eq. (11) is independent from column to column. Therefore, we here discuss just one column of the solution of this equation. For column j , Eq. (11) becomes:

$$\frac{d^2 \psi_{ij}(t)}{dt^2} = \sum_{k=1}^3 \left(A_{ik}(t) \psi_{kj}(t) + B_{ik}(t) \frac{d\psi_{kj}(t)}{dt} \right) + G_{ij}(t) \quad (12)$$

with the initial values as

$$\begin{pmatrix} \psi_{ij}(t_0) \\ \dot{\psi}_{ij}(t_0) \end{pmatrix} = \begin{pmatrix} \delta_{ij} \\ \delta_{(i+3)j} \end{pmatrix} \quad \delta_{ij} = \begin{cases} 1 & i = j \\ 0 & i \neq j \end{cases} \quad (i = 1, 2, 3) \quad (13)$$

In order to map the partial derivatives from the current time t to the initial time t_0 , we divide the whole time span into s steps equally. Thus, every step has an interval of $h = (t - t_0)/s$. When the time comes to $t_n = t_0 + nh$, ($n = 1, \dots, s - 1$), according to the rule of the first and second order symmetric derivative under the limit, we have

$$\begin{aligned} \frac{d^2\psi_{ij}(t)}{dt^2} |_{t_n} &= \lim_{h \rightarrow 0} \frac{\psi_{ij}(t_{n+1}) - 2\psi_{ij}(t_n) + \psi_{ij}(t_{n-1}))}{h^2} \\ \frac{d\psi_{ij}(t)}{dt} |_{t_n} &= \lim_{h \rightarrow 0} \frac{\psi_{ij}(t_{n+1}) - \psi_{ij}(t_{n-1}))}{2h} \\ \psi_{ij}(t) |_{t_n} &= \psi_{ij}(t_n), i = 1, 2, 3 \end{aligned} \tag{14}$$

In mathematics, when the interval h gets closer to zero, Eq. (14) becomes more accurate. However, a small interval means a large number of steps, which will increase the computational burden. Therefore, in this paper, we present a couple of intervals to get a reasonable value. Note that the reasonable value of the interval is largely dependent on the satellite altitude, or to be exact, the satellite velocity.

Substituting Eq. (14) into (12), we have

$$\begin{aligned} &\frac{\psi_{ij}(t_{n+1}) - 2\psi_{ij}(t_n) + \psi_{ij}(t_{n-1}))}{h^2} \\ &\approx \sum_{k=1}^3 \left(A_{ik}(t_n)\psi_{kj}(t_n) + B_{ik}(t_n) \frac{\psi_{kj}(t_{n+1}) - \psi_{kj}(t_{n-1}))}{2h} \right) + G_{ij}(t_n) \end{aligned} \tag{15}$$

where $i = 1, 2, 3$ and $n = 1, \dots, s - 1$. For $i = 1, 2, 3$ and the sequential number n , there are three equations and three unknowns of time t_{n+1} , so that the initial value problem has a unique solution.

To have a better readability, we exchange some terms in Eq. (15), and the alternate form of Eq. (15) can be written as

$$\begin{aligned} &\left(\frac{E}{h^2} - \frac{B(t_n)}{2h} \right) \begin{pmatrix} \psi_{1j}(t_{n+1}) \\ \psi_{2j}(t_{n+1}) \\ \psi_{3j}(t_{n+1}) \end{pmatrix} \approx \left(\frac{2E}{h^2} + A(t_n) \right) \begin{pmatrix} \psi_{1j}(t_n) \\ \psi_{2j}(t_n) \\ \psi_{3j}(t_n) \end{pmatrix} \\ &- \left(\frac{E}{h^2} + \frac{B(t_n)}{2h} \right) \begin{pmatrix} \psi_{1j}(t_{n-1}) \\ \psi_{2j}(t_{n-1}) \\ \psi_{3j}(t_{n-1}) \end{pmatrix} + \begin{pmatrix} G_{1j}(t_n) \\ G_{2j}(t_n) \\ G_{3j}(t_n) \end{pmatrix} \end{aligned} \tag{16}$$

The calculation of the initial steps are as follows

$$\begin{aligned} \psi_{ij}(t_0) &= \psi_{ij}(t_0) \\ \psi_{ij}(t_1) &= \psi_{ij}(t_0) + h\dot{\psi}_{ij}(t_0) \end{aligned} \tag{17}$$

In this way, this equation can be solved. Furthermore, the solutions of Eq. (11), as well as Eq. (5) can be obtained by solving all columns in the same way. Note that the velocity vector can be calculated using the symmetric derivative rule in Eq. (14).

3.2. Difference quotient method

The key idea of the difference quotient algorithm for the state transition matrix computation is to difference two nearby orbits. The most outstanding feature of the algorithm is the simplified structure, which is easy for the computer programming, while the disadvantage is the high time consumption, especially when the number of force model parameters increases.

The expression of the algorithm is quite simple and can be shown as follows:

$$\Phi(t, t_0) = \frac{\partial \vec{X}(t)}{\partial \vec{X}(t_0)} = \lim_{\Delta X_0 \rightarrow 0} \frac{\vec{X}(t, t_0, X_0 + \Delta X_0) - \vec{X}(t, t_0, X_0)}{\Delta X_0} = \Phi_{\Delta}(t, t_0) \tag{18}$$

where $\vec{X}(t, t_0, X_0 + \Delta X_0)$ is the state vector at time t and can be integrated from the initial state \vec{X}_0 at time t_0 . ΔX_0 is the increment state at the initial time while $\Phi_{\Delta}(t, t_0)$ is the result of the difference quotient algorithm for STM. According to the definition of the state transition matrix, $\Phi_{\Delta}(t, t_0)$ will converge to $\Phi(t, t_0)$ under the condition that ΔX_0 approaches to zero. As a rule of thumb, $\Delta X_0 = \sigma_x/100$ is suggested in Hu et al. (2000) where σ is the a priori error of the parameter.

The key of the method is to integrate the state at time t from a different initial state which is $\vec{X}(t_0, t_0, X_0 + \Delta X_0)$. The procedures are presented below according to Hu et al. (2000).

- (a) Integrating the state from $\vec{X}(t_0, t_0, X_0)$ to $\vec{X}(t, t_0, X_0)$, storing in the temporary file ORBIT0;
- (b) Changing the initial state to $\vec{X}(t_0, t_0, X_0 + \Delta X_0)$, for instance, ΔX_0 may be the increment of x component, then integrating it to obtain the state at time t , storing in the file ORBIT1;
- (c) Then making difference of the two orbits, i.e., ORBIT0 and ORBIT1, obtaining the derivatives of $\partial \vec{r} / \partial \vec{x}_0, \partial \dot{\vec{r}} / \partial \vec{x}_0$;
- (d) Repeating procedures (b) and (c), changing the increment component from x to y and z as well as the velocity components and force model parameters to obtain the other derivatives.

4. Validation methodology

The performance of the numerical algebra solution is evaluated in terms of computational cost and accuracy, which is compared with that of the integration and difference quotient method. The computational time consumption may be different depending on the computer, code and programmer skills. However, it is the comparative performance that illustrates the efficiency. In this case, a regular PC with Intel Core i7 processor of 3.60 GHz is used to evaluate the calculation performance for the simulated data of 24 h.

As for the accuracy comparison, the orbit determination of the low earth orbit satellite GRACE (Gravity Recovery and Climate Experiment) (Kang et al., 2003; Tapley et al., 2004b; Jäggi et al., 2007), is performed for the real-time and post processing. It should be noted that the Kalman filtering is represented as real-time processing while batch estimation as post processing in this paper for the sake of simplicity.

Table 1
State of GRACE satellite at initial time.

Serial number	Cartesian	Value	Keplerian	Value
1	x_0 (m)	2728506.247	Semi mayor axis (km)	6834.916
2	y_0 (m)	−3517156.991	Eccentricity	0.0012442
3	z_0 (m)	−5191100.658	Inclination (deg)	88.972
4	V_{x_0} (m/s)	3713.054	Argument of perigee (deg)	64.286
5	V_{y_0} (m/s)	−4442.911	RAAN ^a (deg)	309.003
6	V_{z_0} (m/s)	4973.3210	Mean anomaly (deg)	246.447

^a RAAN represents right ascension of the ascending node.

The initial state of GRACE satellite in conventional inertial system for the simulation is presented in Table 1 where both Cartesian coordinates and corresponding Keplerian elements are shown. The initial epoch is 2010/07/26 00:00:00 UTC time.

From Table 1, we can see that the GRACE satellite orbit is an almost circular, near polar (inclination $\approx 89^\circ$) orbit with an altitude of about 464 km at this epoch.

The simulation strategies of Kalman filtering and batch estimation are shown in Table 2. GPS (Global Positioning System) observations from the GRACE on-board receiver are simulated to determine the state of the satellite. The major difference between the simulated data and real collected data lies in the fact that the simulated data is free from most of the error sources, such as the clock offsets, ionosphere delay and even the ambiguity problems. As a consequence, the precision of the GNSS observations become controllable by adding noises of different level. For example, in the Kalman filtering, decimeter level noise is added to the precise satellite-receiver range while millimeter level noise is added to the range for the batch estimation. The reason is that the orbit determination requirement for the real-time processing is lower than the post processing (Gill et al., 2000; Montunbruck, 2000). Applications of post processing are often related to the determination of geodetic parameters, such as terrestrial/celestial reference frame, plate motion, polar motion, to name but a few, which require even millimeter accuracy (Beutler et al., 1999; Altamimi et al., 2002; Jin and Zhu, 2003; Jin and Park, 2007; Jin et al., 2010). So we simulate the code and carrier phase observables with different-level

measurement noise (only) for real-time and post processing, respectively.

For a low earth orbit satellite, e.g., GRACE, the main perturbations are the earth's gravity, atmosphere drag, third-body effects and solar radiation effects (Seeber, 2003). Thus, these dominant perturbations are considered in the simulation. Besides, some different strategies for the Kalman filtering and batch estimation, such as the gravity model and numerical integrator are shown in Table 2. The reason is that the execution time and memory considerations pose severe restrictions on the on-board real-time applications while these are not problems for the post processing. As a result, the on-board real-time processing should be simple enough to save the on-board resources, without sacrificing the necessary orbit determination requirements.

5. Results

5.1. Time consumption comparison

The computational cost of the real-time and post processing is presented in Tables 3 and 4. The calculations are performed for a period of 24 h with an interval from 60 s to 1 s.

From Table 3, we can see that for the real-time processing, the processing time is largest for the smallest time interval. Besides, as the interval gets larger, the time needed for calculation becomes smaller for all the three methods. In detail, we find that the time cost of algebra solution is about 60% of the integration method on average.

Table 2
Simulation strategies for real-time and post-processed orbit determination of GRACE satellite.

Strategies	Kalman filtering	Batch estimation
Tracking data	GRACE with GPS observations	Same as left
Observation	Code	Phase
Elevation	10 degree above horizon	Same as left
Estimator & Integrator	EKF/RK (4)	LS/RKF7 (8)
Sampling interval	60, 30, 15, 5, 1 s	Same as left
Gravity model	JGM3 50 × 50 (Tapley et al., 1996)	JGM3 70 × 70
Atmosphere drag	Harris-Priester (Harris and Priester, 1963)	Same as left
Solar radiation effects	Cannonball (Lucchesi, 2001)	Same as left
Third-body effects	Consider	Same as left
Simulated Noise	Code: 0.3 m	Phase: 0.003 m

Table 3
Real-time processing time for calculation of STM with GRACE satellite for 24 h.

Interval (s)	CPU TIME (s)		
	Algebra	Difference	Integration
60	30.6	22.8	38.4
30	54.2	50.9	98.4
15	61.9	70.9	89.9
5	71.9	134.8	125.1
1	349.9	601.2	582.1

Table 4
Post processing time for calculation of STM with GRACE satellite for 24 h.

Interval (s)	CPU TIME (s)		
	Algebra	Difference	Integration
60	12.3	71.5	41.2
30	37.8	122	46.6
15	58.3	341.7	204.7
5	84.5	648.9	231.7
1	415.6	2193.7	1155.5

For the post processing, Table 4 shows that the time cost of algebra solution is the least among all the cases, followed by the integration and difference quotient method. Generally speaking, the time cost of algebra solution is about 40% of the integration method and 20% of the difference quotient method.

In summary, the numerical algebra solution has obvious advantages over the other two solutions with regard to the time consumption.

5.2. Orbit determination accuracy comparison

In this section, we will demonstrate whether the accuracy of algebra solution can meet the demand for the orbit determination or not. The demonstration is divided into two parts which are the real-time and post processing parts while the estimated parameters are the position and velocity components of the satellite.

As mentioned in the introduction part, the integration method is the most accurate solution of STM and also taken as a reference to the other solutions in this paper. Note that in the following tables, the abbreviation “A-I” stands for the difference between algebra and integration solution while “D-I” represents the difference between difference quotient and integration method.

Table 5
Orbit error and RMS difference of orbit in one day for the real-time processing.

Interval (s)	Position error (m)	RMS difference position (m)		Velocity error (m/s)	RMS difference velocity (m/s)	
		A-I	D-I		A-I	D-I
		60	1.398		1.04E-03	1.33E-05
30	1.238	2.37E-04	6.34E-06	1.211E-03	6.34E-06	4.45E-09
15	1.202	5.68E-05	3.13E-06	1.186E-03	3.13E-06	8.64E-09
5	1.180	6.29E-06	1.04E-06	1.170E-03	1.04E-06	2.55E-08
1	1.176	2.50E-07	2.08E-07	1.168E-03	2.08E-07	9.85E-08

5.2.1. Kalman filtering estimation

In the real-time processing, the orbit can be determined every epoch by Kalman filtering. The results of orbit determination are presented in Table 5 which include the orbit error of integration solution and the root mean square (RMS) difference of algebra and difference quotient solution with regard to the integration solution. The RMS difference of position $\Delta\sigma$ is calculated by the following formula while the corresponding RMS difference of velocity is computed in the same way.

$$\Delta\sigma = \left\{ \frac{1}{N} \sum_{i=1}^N [(x_i^J - x_i^I)^2 + (y_i^J - y_i^I)^2 + (z_i^J - z_i^I)^2] \right\}^{1/2} \tag{19}$$

where (x_i, y_i, z_i) are the three position components of Cartesian coordinate system at step i . The superscript I means the integration solution and J stands for the solution of algebra or difference quotient while N is the total amount of the steps for the numerical method.

From Table 5, we can see that the position error is about 1.2 m and velocity error is about 1.2 mm/s. When the interval is 60 s, the position RMS difference of the numerical algebra solution with respect to the numerical integration method is about 1.04 mm while the position error of the numerical integration method is about 1.20 m. Meanwhile, the RMS difference of the orbit between the algebra and difference quotient solution becomes smaller with the decrease of the interval, which means that the accuracy of these solutions gets better.

Taking the accuracy of the observables into account, the position error of the integration method should be above decimeter due to the decimeter-level noise of the observables, which is actually around 1.2 m as shown in Table 5. From this point of view, the position difference between algebra and integration solution under decimeter is indistinguishable.

Furthermore, the orbit errors of the integration method, as well as the orbit differences between algebra and integration methods every epoch are presented in Fig. 1. The interval of the following result is 60 s, which represents the worst performance case in this paper.

The top panel of Fig. 1 illustrates the orbit errors of the numerical integration method while the bottom panel presents the orbit differences between algebra and integration solution.

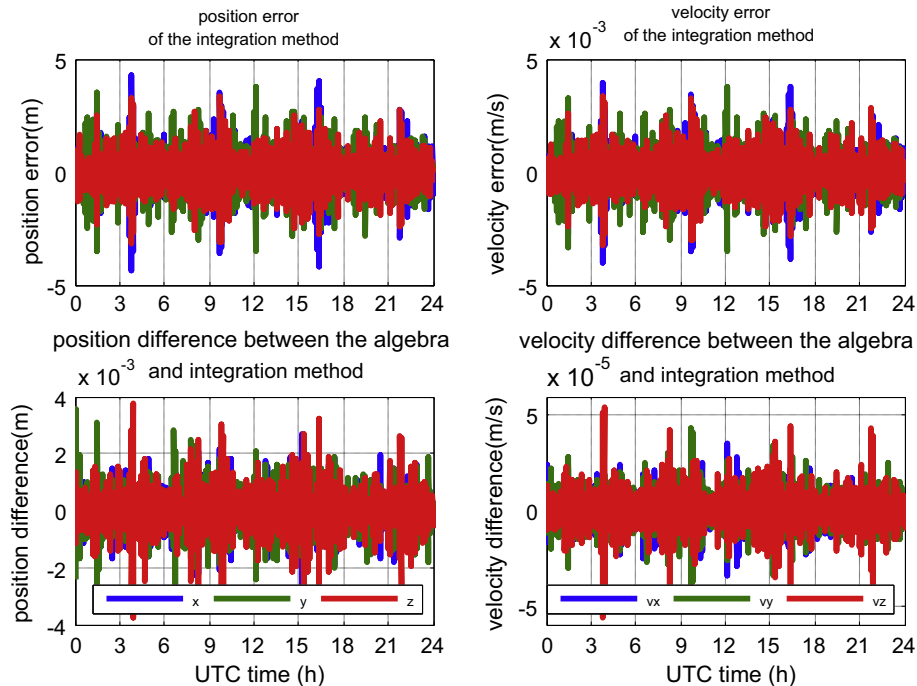


Fig. 1. The orbit errors of the integration method and the corresponding differences between algebra and integration method every epoch in the case of real-time processing with 60-s interval for 24 h.

As the top-left panel of Fig. 1 shows, the position errors are ranged from -2 to 2 m in most of the time. There exist some large errors in some epochs and the reason may be the low quality of the observations or large geometric dilution of precision (GDOP) value.

The bottom-left panel of Fig. 1 illustrates that the position differences are ranged from -4 to 4 mm. As the position error is at the level of about 1.2 m, this mm-level difference can be neglected.

Meanwhile, the right panel of Fig. 1 presents the performance of velocity solution, which shows similar results as the performance of position solution in the left panel. The velocity differences between algebra and integration solution are less than 2 orders of magnitude of the velocity error, as shown in Table 5.

Therefore, in the worst performance case of algebra solution, the orbit differences between algebra and integra-

tion methods are small enough to be neglected. Thus, the algebra solution is qualified for the real-time processing.

5.2.2. Batch estimation

In the post processing, the procedure is quite different from that of real-time processing. Instead of yielding sequential state estimates every epoch, the initial state corrections need to be computed using a full set of observations by the batch least square estimation. Therefore, the results of the initial state corrections of these methods are presented and compared with each other firstly as follows.

The results in Tables 6 and 7 represent the worst and best performance of the algebra solution comparing with the integration method when the interval is 60 s and 1 s, respectively. From Table 6, we can see that the initial state correction difference between the algebra and integration solution is 2 orders of magnitude lower than the correction.

Table 6
Initial state corrections by batch estimation with 60-s interval.

Method	Δx_0 (m)	Δy_0 (m)	Δz_0 (m)	ΔV_{x_0} (m/s)	ΔV_{y_0} (m/s)	ΔV_{z_0} (m/s)
Integration	2.03E-04	1.98E-04	1.51E-05	-3.51E-07	-3.47E-07	7.00E-09
A-I	7.46E-06	-3.82E-06	7.64E-06	-1.20E-08	1.20E-09	1.11E-08
D-I	-2.21E-07	3.10E-07	-3.03E-07	3.00E-10	-3.00E-10	-4.00E-10

Table 7
Initial state corrections by batch estimation with 1-s interval.

Method	Δx_0 (m)	Δy_0 (m)	Δz_0 (m)	ΔV_{x_0} (m/s)	ΔV_{y_0} (m/s)	ΔV_{z_0} (m/s)
Integration	-2.81E-05	3.68E-05	-5.09E-05	9.76E-08	3.14E-08	-5.98E-08
A-I	-3.80E-09	4.40E-09	-4.50E-09	0.00E+00	0.00E+00	0.00E+00
D-I	1.87E-07	-1.60E-07	9.30E-08	-1.00E-10	2.00E-10	1.00E-10

When the interval is 1 s, the magnitude of the difference decreases to 4 orders lower than the correction, and algebra solution outperforms the difference quotient solution as Table 7 presented.

In order to testify the effects of these small differences as well as STM on precise orbit determination, the following formula is adopted to compute the state correction.

$$\Delta S_i = \Phi(t_i, t_0)\Delta S_0 \tag{20}$$

where $\Phi(t_i, t_0)$ is the state transition matrix, ΔS_0 is the estimated initial state correction and ΔS_i is the state correction at step i with $\Delta S_i = (\Delta x_i, \Delta y_i, \Delta z_i, \Delta V_{x_i}, \Delta V_{y_i}, \Delta V_{z_i})$. The definitions of RMS difference of the orbit are the same as given in Eq. (19) and the results are shown as follows.

From Table 8, we can find that the orbit RMS difference of the algebra and integration solution gets closer when the intervals become smaller. When the interval is 60 s, the position RMS difference of the numerical algebra solution with respect to the numerical integration method is about

0.01 mm while the position error of the numerical integration method is about 0.30 mm.

As well, the position and velocity errors of the integration method, as well as the orbit differences between the algebra and integration methods every epoch are shown in Fig. 2, in which the interval is 60 s, representing the worst performance for post-processed orbit determination.

The left panel of Fig. 2 shows the position errors and differences between algebra and integration solution, and the right panel presents the corresponding performance of the velocity.

From Fig. 2, we can see that the position errors and differences have a clear period of about 1.5 h which coincide with the revolution period of GRACE satellite. From the left panel, we find that the position differences between algebra and integration solution are about an order of magnitude lower than the position error which is shown in Table 8. The same conclusion can be drawn for the comparisons of the velocity performances. Meanwhile, from

Table 8
Orbit error and RMS difference of orbit in one day for post processing.

Interval (s)	Position error (mm)	RMS difference position (mm)		Velocity error (mm/s)	RMS difference velocity (mm/s)	
		A-I	D-I		A-I	D-I
60	0.340	1.24E-02	2.09E-04	3.75E-04	1.33E-05	2.37E-07
30	0.290	6.28E-03	3.42E-04	3.17E-04	6.94E-06	3.63E-07
15	0.214	1.40E-03	3.35E-04	2.28E-04	1.56E-06	3.52E-07
5	0.184	1.23E-04	4.75E-04	1.56E-04	1.34E-07	5.31E-07
1	0.067	4.29E-06	1.64E-04	7.33E-05	7.25E-09	1.80E-07

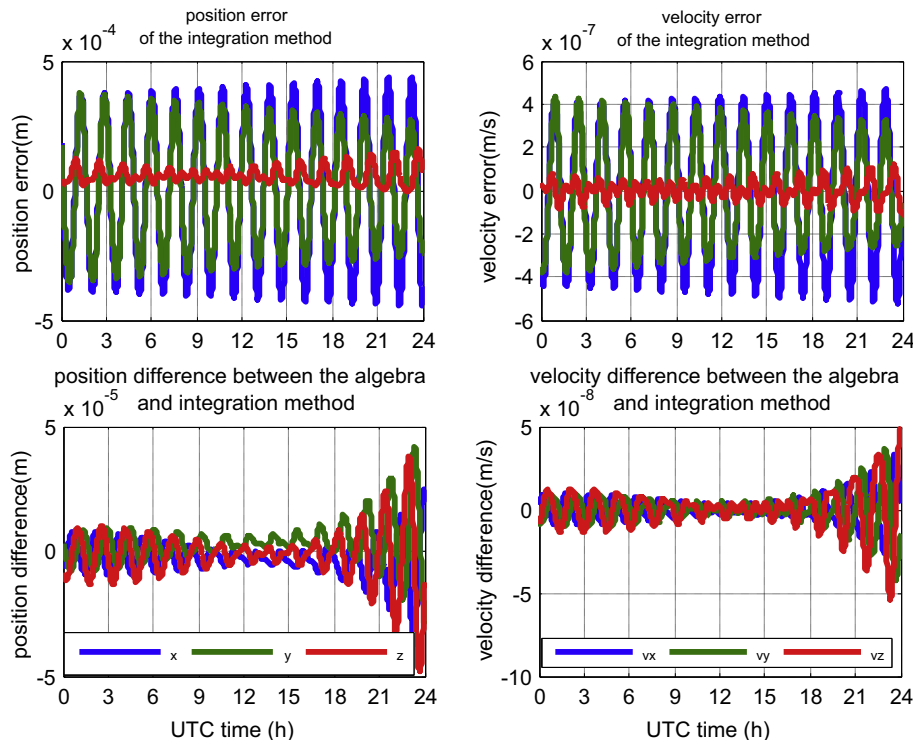


Fig. 2. The orbit errors of the integration method and the corresponding differences between algebra and integration method every epoch in the case of post processing with 60-s interval for 24 h.

the bottom panel, we find that the position differences increase rapidly after about 20 h, which means that some errors accumulated in the algebra solution for post processing.

As we can see from Fig. 2, the position differences are ranged from -0.05 to 0.05 mm while the position error is about 0.3 mm as presented in Table 8, which means that the position differences are still smaller than the position error. Thus, the precision of algebra solution can still be accepted.

From the above analyses, the availability of algebra solution for the real-time and post-processed orbit determination are demonstrated in a simulation manner. In practice, a smaller interval may be used, especially for the real-time processing, which means that the algebra solution can have a better performance than that shown in Figs. 1 and 2. Therefore, further studies will be required to determine orbit accuracy for real missions. Advantageously, the time consumption of the algebra solution is almost the least among the three investigated methods, which is particularly beneficial to the real-time orbit determination.

6. Conclusion

In this paper, a new algorithm named the numerical algebra solution for the state transition matrix is presented. Compared with the other numerical solutions, the most outstanding feature of the proposed method is that it costs the least computation time while maintains a comparable accuracy for both real-time and post-processed orbit determination.

It shows that the time consumption of the algebra solution is about 60% and 40% of the integration method for real-time and post processing, respectively. Furthermore, for the real-time orbit determination, the maximum RMS difference of position between algebra and integration solution is 1.04 mm while the position error is about 1.20 m. Meanwhile, for the post processing, the maximum RMS difference of position is 0.01 mm while the position error is about 0.30 mm. These accuracy comparisons demonstrate that the difference between algebra and integration solution is indistinguishable and can be accepted in the orbit determination.

Therefore, the results have shown the possibility, availability and potentiality of the algebra solution when applied in orbit determination. However, these conclusions are based on the simulation and we are aware of the limitations of the simulations. To validate the orbit determination accuracy and computational efficiency with real collected data is our mission of the next stage.

Acknowledgement

The study is funded by National Key Research and Development Program of China (2016YFB0501900,

2016YFB0501902), National Natural Science Foundation of China (41574025, 41574013, 41274042) and State Key Laboratory of Geo-information Engineering (SKLGIE2015-M-2-2). We would like to thank the editor and three anonymous reviewers for very valuable comments that significantly improve the quality of this manuscript.

References

- Altamimi, Z., Boucher, C., Sillard, P., 2002. New trends for the realization of the International Terrestrial Reference System. *Adv. Space Res.* 30 (2), 175–184. [http://dx.doi.org/10.1016/S0273-1177\(02\)00282-X](http://dx.doi.org/10.1016/S0273-1177(02)00282-X).
- Battin, R.H., 1964. *Astronautical Guidance*. McGraw-Hill, New York.
- Beutler, G., Rothacher, M., Schaer, S., Springer, T.A., Kouba, J., Neilan, R.E., 1999. The International GPS Service (IGS): an interdisciplinary service in support of earth sciences. *Adv. Space Res.* 23 (4), 631–653. [http://dx.doi.org/10.1016/S0273-1177\(99\)00160-X](http://dx.doi.org/10.1016/S0273-1177(99)00160-X).
- Beutler, G., 2004. *Methods of Celestial Mechanics: Volume I: Physical, Mathematical, and Numerical Principles*. Springer Science & Business Media. Berlin Heidelberg. <http://dx.doi.org/10.1007/b138225>.
- Born, G.H., Kirkpatrick, J.C., 1970. Application of Brouwer's artificial-satellite theory to computation of the state transition matrix. NASA Johnson Space Center, NASA TN D-5934. Last accessed 2016/10/17. <<http://ntrs.nasa.gov/archive/nasa/casi.ntrs.nasa.gov/19700027253.pdf>>.
- Broucke, R.A., 1970. On the matrizant of the two-body problem. *Astron. Astrophys.* 6, 173–182.
- Der, G.J., 1997. An elegant state transition matrix. *J. Astronaut. Sci.* 45 (4), 371–390. <http://dx.doi.org/10.2514/6.1996-3660>.
- Ditto, F.H., 1969. Partial derivatives used in trajectory estimation. *Celestial Mech.* 1 (1), 130–140. <http://dx.doi.org/10.1007/BF01230638>.
- Gill, E., Montenbruck, O., Brieß, K., 2000. GPS-based autonomous navigation for the BIRD satellite. In: 15th International Symposium on Spaceflight Dynamics, 26–30 June 2000, Biarritz, France. Last accessed 2016/10/18. <http://www.dlr.de/rb/Portaldata/38/Resources/dokumente/GSOC_dokumente/RB-RFT/ISSFD_XV31.pdf>.
- Goodyear, W.H., 1965. Completely general closed-form solution for coordinates and partial derivative of the two-body problem. *Astronom. J.* 70, 189–192. <http://dx.doi.org/10.1086/109713>.
- Harris, I., Priester, W., 1963. Relation between theoretical and observational models of the upper atmosphere. *J. Geophys. Res.* 68 (20), 5891–5894. <http://dx.doi.org/10.1029/JZ068i020p05891>.
- Hu, X., Huang, C., Liao, X., 2000. The difference algorithm for state transition matrix and its applications. *Acta Astronomica Sinica* 41, 113–122. <http://dx.doi.org/10.15940/j.cnki.0001-5245.2000.02.001>.
- Jäggi, A., Hugentobler, U., Bock, H., Beutler, G., 2007. Precise orbit determination for GRACE using undifferenced or doubly differenced GPS data. *Adv. Space Res.* 39 (10), 1612–1619. <http://dx.doi.org/10.1016/j.asr.2007.03.012>.
- Jin, S., Zhu, W., 2003. International Terrestrial Reference Frame: current status and its future. *Prog. Astron.* 21 (3), 241–249.
- Jin, S., Park, P.H., 2007. Tectonic activities and deformation in South Korea constrained by GPS observations. *International Journal of Geology*, 2, pp.11–15. Last accessed 2016/10/18. <http://center.shao.ac.cn/geodesy/publications/Jin_2007IJG.pdf>.
- Jin, S., Chambers, D.P., Tapley, B.D., 2010. Hydrological and oceanic effects on polar motion from GRACE and models. *J. Geophys. Res.: Solid Earth* 115, B02403. <http://dx.doi.org/10.1029/2009JB006635>.
- Jin, S. (Ed.), 2012. *Global Navigation Satellite Systems: Signal, Theory and Applications*. InTech-Publisher, Rijeka, Croatia.
- Junkins, J.L., Majji, M., Turner, J.D., 2008. High Order Keplerian State Transition Tensors. In: Crassidis, J.L., Junkins, J.L., Howell, K.C., Oshman, Y., Thienel, J.K. (Eds.), *Proceedings of the F. Landis Markley Astronautics Symposium*. AAS, Cambridge, Maryland.

- Kang, Z., Nagel, P., Pastor, R., 2003. Precise orbit determination for GRACE. *Adv. Space Res.* 31 (8), 1875–1881. [http://dx.doi.org/10.1016/S0273-1177\(03\)00159-5](http://dx.doi.org/10.1016/S0273-1177(03)00159-5).
- Liu, L., 2000. *Orbit Theory of Spacecraft*. National Defense Industry Press, Beijing.
- Lucchesi, D.M., 2001. Reassessment of the error modelling of non-gravitational perturbations on LAGEOS II and their impact in the Lense-Thirring determination. Part I. *Planet. Space Sci.* 49 (5), 447–463. [http://dx.doi.org/10.1016/S0032-0633\(00\)00168-9](http://dx.doi.org/10.1016/S0032-0633(00)00168-9).
- Montenbruck, O., 2000. An epoch state filter for use with analytical orbit models of low earth satellites. *Aerosp. Sci. Technol.* 4 (4), 277–287. [http://dx.doi.org/10.1016/S1270-9638\(00\)00133-4](http://dx.doi.org/10.1016/S1270-9638(00)00133-4).
- Montenbruck, O., Gill, E., 2000. *Satellite orbits: models, methods and applications*. Springer Science & Business Media, Berlin Heidelberg. <http://dx.doi.org/10.1007/978-3-642-58351-3>.
- Mueller, A.C., 1977. An analytical state transition matrix for orbits perturbed by an oblate spheroid. ACM Technical Report. ACM-TR-104. Last accessed 2016/10/17. <<https://ntrs.nasa.gov/archive/nasa/casi.ntrs.nasa.gov/19780007194.pdf>>.
- Peter, D.L., Maria, S.T., 2014. *Calculus with Applications*, second ed. Springer, New York.
- Ramachandran, M.P., 2015. Approximate state transition matrix and secular orbit model. *Int. J. Aerosp. Eng.* 2015, 6. <http://dx.doi.org/10.1155/2015/475742> Article ID 475742.
- Seeber, G., 2003. *Satellite Geodesy: Foundations, Methods, and Applications*. Walter de Gruyter, New York.
- Shepperd, S.W., 1985. Universal Keplerian state transition matrix. *Celestial Mech.* 35 (2), 129–144. <http://dx.doi.org/10.1007/BF01227666>.
- Tapley, B.D., Ries, J.C., Davis, G.W., Eanes, R.J., Schutz, B.E., Shum, C.K., Watkins, M.M., Marshall, J.A., Nerem, R.S., Putney, B.H., Klosko, S.M., 1994. Precision orbit determination for TOPEX/POSEIDON. *J. Geophys. Res.: Oceans* 99 (C12), 24383–24404. <http://dx.doi.org/10.1029/94JC01645>.
- Tapley, B.D., Watkins, M.M., Ries, J.C., Davis, G.W., Eanes, R.J., Poole, S.R., Rim, H.J., Schutz, B.E., Shum, C.K., Nerem, R.S., Lerch, F.J., 1996. The joint gravity model 3. *J. Geophys. Res.: All Series* 101, 28–029. <http://dx.doi.org/10.1029/96JB01645>.
- Tapley, B.D., Schutz, B.E., Born, G.H., 2004a. *Statistical Orbit Determination*. Elsevier Academic Press, Amsterdam.
- Tapley, B.D., Bettadpur, S., Watkins, M., Reigber, C., 2004b. The gravity recovery and climate experiment: mission overview and early results. *Geophys. Res. Lett.* 31 (9). <http://dx.doi.org/10.1029/2004GL019920>.
- Willis, P., Haines, B., Bar-Sever, Y., Bertiger, W., Muellerschoen, R., Kuang, D., Desai, S., 2003. TOPEX/Jason combined GPS/DORIS orbit determination in the tandem phase. *Adv. Space Res.* 31 (8), 1941–1946. [http://dx.doi.org/10.1016/S0273-1177\(03\)00156-X](http://dx.doi.org/10.1016/S0273-1177(03)00156-X).
- Willis, P., Fagard, H., Ferrage, P., Lemoine, F.G., Noll, C.E., Noomen, R., Otten, M., Ries, J.C., Rothacher, M., Soudarin, L., Tavernier, G., 2010. The international DORIS service (IDS): toward maturity. *Adv. Space Res.* 45 (12), 1408–1420. <http://dx.doi.org/10.1016/j.asr.2009.11.018>.
- Xu, G., 2007. *GPS: Theory, Algorithms and Applications*, second ed. Springer Science & Business Media, Berlin Heidelberg.
- Xu, G., Xu, J., 2013. *Orbits: 2nd Order Singularity-free Solutions*, second ed. Springer Science & Business Media, Berlin Heidelberg.